Author Manuscript

Author Manuscript

Author Manuscript

Author Manuscript

HHS Public Access

Author manuscript

Nat Cell Biol. Author manuscript; available in PMC 2014 January 01.

Published in final edited form as:

Nat Cell Biol. 2013 July ; 15(7): 846–852. doi:10.1038/ncb2766.

Bmi1 represses *Ink4a/Arf* and *Hox* genes to regulate stem cells in the rodent incisor

Brian Biehs[1,2,*,†], **Jimmy Kuang-Hsien Hu**[1,*], **Nicolas B. Strauli**[1], **Eugenio Sangiorgi**[3], **Heekyung Jung**[4], **Ralf-Peter Heber**[1], **Sunita Ho**[5], **Alice F. Goodwin**[1], **Jeremy S. Dasen**[4], **Mario R. Capecchi**[3], and **Ophir D. Klein**[1,2,‡]

[1]Department of Orofacial Sciences and Program in Craniofacial and Mesenchymal Biology, University of California San Francisco, San Francisco, CA 94143, USA

[2]Department of Pediatrics and Institute for Human Genetics, University of California San Francisco, San Francisco, CA 94143, USA

[3]Howard Hughes Medical Institute and Department of Human Genetics, University of Utah School of Medicine, Salt Lake City, UT 84112, USA

[4]Smilow Neuroscience Program, Department of Physiology and Neuroscience, Howard Hughes Medical Institute, NYU School of Medicine, New York, New York, United States of America

[5]Department of Preventative and Restorative Dental Sciences, University of California San Francisco, San Francisco, CA 94143, USA

Abstract

The polycomb group gene *Bmi1* is required for maintenance of adult stem cells in many organs[1, 2]. Inactivation of *Bmi1* leads to impaired stem cell self-renewal due to deregulated gene expression. One critical target of BMI1 is *Ink4a/Arf*, which encodes the cell cycle inhibitors $p16^{ink4a}$ and $p19^{Arf}$[3]. However, deletion of *Ink4a/Arf* only partially rescues *Bmi1* null phenotypes[4], indicating that other important targets of BMI1 exist. Here, using the continuously-growing mouse incisor as a model system, we report that *Bmi1* is expressed by incisor stem cells and that deletion of *Bmi1* resulted in fewer stem cells, perturbed gene expression, and defective enamel production. Transcriptional profiling revealed that *Hox* expression is normally repressed by BMI1 in the adult, and functional assays demonstrated that BMI1-mediated repression of *Hox* genes preserves the undifferentiated state of stem cells. As *Hox* gene upregulation has also been reported in other systems when *Bmi1* is inactivated[1, 2, 5–7], our findings point to a general mechanism whereby BMI1-mediated repression of *Hox* genes is required for the maintenance of adult stem cells and for prevention of inappropriate differentiation.

Users may view, print, copy, download and text and data- mine the content in such documents, for the purposes of academic research, subject always to the full Conditions of use: http://www.nature.com/authors/editorial_policies/license.html#terms

‡Author for correspondence Ophir.Klein@ucsf.edu – +1-415-476-4719.

*These authors contributed equally.

†Current addresses: Department of Molecular Biology, Genentech Inc., 1 DNA way, South San Francisco, CA 94080, USA (B.B.); Istituto di Genetica Medica, Università Cattolica del Sacro Cuore, Rome, Italy (E.S.)

Author Contributions

B.B., J.K.H., N.B.S., H.J., E.S., R.-P.H., A.G., J.S.D and O.D.K. designed and performed experiments. B.B., J.K.H, and O.D.K. wrote the manuscript. All authors discussed results, analyzed data and edited the manuscript.

Author Manuscript Author Manuscript Author Manuscript Author Manuscript

A central goal in stem cell biology is to understand the mechanisms of tissue regeneration and renewal used by diverse organs. In the case of the rodent incisor, continuous growth relies on stem cells that share several characteristics with other regenerating adult systems[8–11]. These include residence in a discrete niche, slow division kinetics with respect to surrounding cells, and the ability to give rise to differentiated lineages throughout the life of the animal. Label retaining experiments in mice utilizing either BrdU incorporation or genetic labeling with a tetracycline inducible Histone 2B-GFP (H2BGFP) reporter demonstrated that a population of slowly dividing epithelial stem cells was present in a structure called the labial cervical loop (LaCL) at the proximal end of the incisor[8, 12]. Lineage tracing experiments showed that these cells gave rise to the highly proliferative transit-amplifying (T-A) cells that then differentiated into enamel-secreting ameloblasts[11–13]. Genetic analyses have shown that development of the incisor stem cells is controlled by TGF-β/BMP and FGF signaling[9, 10] and that adult stem cells require active SHH signaling to produce differentiated progeny[12]. However, it remains relatively unknown how homeostasis is regulated in the adult LaCL. Because *Bmi1* plays a key role in adult stem cell homeostasis in a number of mammalian tissues[1, 2, 4, 14], we set out to study the role of *Bmi1* in the adult incisor.

To investigate *Bmi1* expression, we utilized $Bmi1^{GFP}$ reporter mice, in which the second exon of *Bmi1* was replaced by GFP, resulting in a null allele[15]. In $Bmi1^{GFP/+}$ adult mice, GFP was expressed in cells of the stellate reticulum (SR) and in the outer enamel epithelium (OEE), where the LaCL stem cells reside (Fig. 1a–c). These cells underwent infrequent cell divisions[12] and thus retained H2B-GFP or BrdU after extended chase periods (Fig. 1b, 2f), similar to stem cells of the hair follicle bulge[16]. In addition, in $Bmi1^{GFP/+};Gli1^{LacZ/+}$ mice, $Bmi1^{GFP}$ was co-expressed with $Gli1^{LacZ}$, a marker for adult dental stem cells[12] (Supplementary Fig. S1a–d). Together, these data suggested that *Bmi1* marks the incisor stem cells.

To determine whether *Bmi1*-expressing cells are indeed stem cells that can give rise to differentiated cell types over a long period of time, we performed inducible genetic lineage tracing. This technique permanently labels a cell and its progeny and definitively identifies adult stem cells *in vivo*[17]. To this end, we genetically labeled *Bmi1*-expressing cells and traced their descendants using an inducible $Bmi1^{CreER}$ strain[18] crossed to a Cre-responsive reporter line (*R26R-Tm-GFP*)[19]. Induction of Cre activity by tamoxifen injection results in permanent expression of GFP in *Bmi1*-expressing cells and their progeny. While we did not detect GFP labeling in uninjected $Bmi1^{CreER/+};R26R\text{-}Tm\text{-}GFP$ mice (Fig. 1d), we observed a few labeled cells in the LaCL and surrounding mesenchyme 3 days after tamoxifen injection (Fig. 1e, insert). GFP was also observed in blood vessels (Fig. 1e, arrowhead), consistent with a previous report of *Bmi1* expression in endothelium[20]. By 7 days after tamoxifen injection, increased numbers of GFP-positive cells were observed in the LaCL and mesenchyme (Fig. 1f). Importantly, as cells in the pre-ameloblast region move ~350 μm per day[21, 22], the appearance of GFP-positive pre-ameloblasts in the dental epithelium (Fig. 1f, arrow) several days after tamoxifen injection established the production of differentiated cells from *Bmi1*-positive progenitors. Longer chases revealed the accumulation of labeled cells in the LaCL, indicating that LaCL stem cells had undergone self-renewal (Fig. 1g,h).

Author Manuscript Author Manuscript Author Manuscript Author Manuscript

The appearance of groups of labeled ameloblasts suggested that each cluster represented the progeny of a single stem cell whose descendants underwent several rounds of replication. Together, the expression and lineage tracing data demonstrated that *Bmi1*-expressing cells in the LaCL are stem cells.

Next, to identify the function of *Bmi1* in the mouse incisor, we analyzed the architecture of the dental epithelium in *Bmi1* null animals (*Bmi1*$^{GFP/GFP}$, hereafter referred to as *Bmi1*$^{-/-}$) at 5 months of age by performing haematoxylin and eosin staining. *Bmi1*$^{-/-}$ animals had LaCLs that were consistently thinner in both the sagittal and coronal planes, with a substantial decrease in the amount of SR compared to *Bmi1*$^{+/+}$ siblings (Fig. 2a,h). To obtain a clearer picture of the morphological defect in *Bmi1*$^{-/-}$ LaCLs, we prepared 3D reconstructions of the LaCL from *Bmi1*$^{+/+}$ and *Bmi1*$^{-/-}$ animals. The 3D reconstructions demonstrated a significant loss of tissue in the LaCL, specifically in the SR on the labial side (Fig. 2b,i, and Supplementary Fig. S2). On average, *Bmi1*$^{-/-}$ LaCLs showed a 28% decrease in total volume compared to controls (Fig. 2v).

We then asked if the expression profile was altered in *Bmi1*$^{-/-}$ LaCLs by analyzing markers of dental epithelium. E-cadherin is normally expressed in stem cells residing in the SR and OEE and downregulated in the T-A zone[21] (Fig. 2c). Conversely, P-cadherin is absent in the stem cell region but upregulated in the T-A region[21] (Fig. 2e). In *Bmi1*$^{-/-}$ LaCLs, the domain of E-cadherin expression was smaller (Fig. 2j), and P-cadherin staining was expanded posteriorly into the OEE (Fig. 2l, asterisk), indicating that cells in this region assumed a more differentiated character. We next examined the expression of integrin alpha 6 (ITGA6), a marker of hematopoietic[23], neural[23], tracheal[24], and epidermal[25] stem cells that is also expressed in the dental epithelial stem cells[26]. Similar to E-cadherin, ITGA6 is normally expressed in the SR and OEE of the LaCL (Fig. 2d), and its domain of expression was dramatically smaller in the LaCL of *Bmi1*$^{-/-}$ animals (Fig. 2k). Together, the expression pattern of these markers indicated that a loss of *Bmi1* activity caused a reduction in the size of the stem cell-containing region in the incisor.

Because *Bmi1* is known to regulate stem cell self-renewal[1, 2, 4], we asked whether the reduction of cells in the *Bmi1*$^{-/-}$ LaCLs was due at least in part to a reduced population of stem cells, using BrdU label retention as a marker of these cells[8, 12]. We administered BrdU to perinatal *Bmi1*$^{+/+}$ and *Bmi1*$^{-/-}$ pups and analyzed the number of label-retaining cells (LRCs) in 6-week-old adult mice (Fig. 2f,m). On average, *Bmi1*$^{-/-}$ LaCLs had 45% fewer LRCs compared to *Bmi1*$^{+/+}$ controls (Fig. 2w), indicating that *Bmi1* regulates stem cell number in the incisor. Similarly low levels of apoptosis were observed in the mutants and controls (Supplementary Fig. S1e,f).

Finally, as *Bmi1*-expressing stem cells give rise to enamel-secreting ameloblasts, we compared the mineralized enamel in *Bmi1*$^{+/+}$ and *Bmi1*$^{-/-}$ lower incisors using microtomography scans (microCT). In 5-month-old *Bmi1*$^{+/+}$ adults, mature enamel was present in a swath that extended from a region proximal to the molars to the distal tip of the tooth (Fig. 2g). In contrast, mature *Bmi1*$^{-/-}$ enamel receded to a position between the proximal and distal roots of the first molar, indicating defective enamel formation by *Bmi1*$^{-/-}$ progeny (Fig. 2n).

Author Manuscript Author Manuscript Author Manuscript Author Manuscript

In other contexts, BMI1 and other polycomb group proteins preserve stem cell self-renewal through repression of the *Ink4a/Arf* locus, which encodes two tumor suppressor proteins that negatively regulate the cell cycle[1, 3, 4]. As *Ink4a/Arf* was also upregulated in the *Bmi1* null incisor epithelium (Fig. 3a), it was possible that BMI1 functions similarly in mouse incisor stem cells by repressing *Ink4a/Arf* expression. To test this possibility and to dissect phenotypes associated with *Ink4a/Arf* upregulation, we bred *Bmi1*$^{-/-}$*;Ink4a/Arf*$^{-/-}$ triple mutants. We first observed that the additional loss of *Ink4a/Arf* was able to restore LaCL volume (Fig. 2o,p,v). *Ink4a/Arf* deletion also partially rescued LRC number (Fig. 2t,w), consistent with the notion that *Bmi1* is required to maintain an adequate population of stem cells for homeostasis by repressing *Ink4a/Arf* expression. However, the incompleteness of the rescue pointed to the existence of additional BMI1 targets that may contribute to the mutant phenotype. Similarly, in other organs, deletion of *Ink4a/Arf* in *Bmi1* null animals was insufficient to completely rescue either the morphological defects[4] or the maintenance of downstream lineage specification[14]. Indeed, the marker expression pattern of the *Bmi1*$^{-/-}$*;Ink4a/Arf*$^{-/-}$ mutant LaCL resembled that of the *Bmi1* null incisor, with diminished E-cadherin and ITGA6 expression in the SR and OEE, accompanied by an expanded P-cadherin domain (Fig. 2q–s), suggesting that *Bmi1* maintains incisor stem cell identity through mechanisms that do not involve *Ink4a/Arf*. Importantly, despite the rescue in LaCL size, *Bmi1*$^{-/-}$*;Ink4a/Arf*$^{-/-}$ mice exhibited defects in enamel deposition (Fig. 2u), a phenotype that is likely due to abnormal gene expression in stem cells and their progeny.

To identify additional BMI1 targets, we performed microarray analysis on dental epithelia from control and *Bmi1* null incisors. In addition to *Ink4a/Arf*, many other genes were upregulated in the mutants, including 9 *Hox* genes from 3 different Hox clusters (Fig. 3a). To validate the upregulation of *Hox* genes in *Bmi1* null dental epithelia, we performed RT-PCR on *Bmi1*$^{+/+}$ and *Bmi1*$^{-/-}$ LaCLs. Whereas *Hoxa7*, *b7*, and *c6* transcripts were undetectable in control LaCLs, their expression was readily detected in *Bmi1*$^{-/-}$ LaCLs (Fig. 3b). Similarly, *Hoxc9* and *a9* expression was dramatically increased in the *Bmi1*$^{-/-}$ LaCLs. Thus, BMI1 suppressed the expression of several *Hox* genes in the LaCL, suggesting that de-repressed *Hox* transcription may lead to premature differentiation. Gene ontology analysis further confirmed this notion, as genes associated with differentiation were upregulated in the mutants (Fig. 3c and Supplementary Table S1). Specifically, genes important for enamel formation that are normally expressed in maturing ameloblasts, such as *amelotin* (*Amtn*) and *kallikrein-related peptidase* (*Klk4*)[27, 28], were prematurely upregulated in the LaCL (Supplementary Table S1).

It was next important to determine if BMI1-mediated repression of *Hox* genes was functionally required for the regulation of adult incisor stem cells. We utilized a tissue culture system[21, 29] to enable concurrent manipulation of *Hox* expression levels in incisor stem cells. LaCL epithelia from *Bmi1*$^{+/+}$ or *Bmi1*$^{-/-}$ incisors were dissociated to create single cell suspensions. 10 days after plating control cells, three morphological types of colonies appeared, with the majority composed of small and tightly packed cells that continued to express E-cadherin, suggesting that they maintained some of the incisor stem cell characteristics (Supplementary Fig. S3a–g). In contrast, dissociated LaCL cells from *Bmi1*$^{-/-}$ incisors grew very poorly and produced far fewer colonies (Supplementary Fig.

Author Manuscript Author Manuscript Author Manuscript Author Manuscript

S3h), consistent with upregulation of *Ink4a/Arf* and the self-renewal defects described above, but no change in apoptosis was observed in cultured *Bmi1*$^{-/-}$ cells (Supplementary Fig. S1g,h). Finally, sorting of cells from *Bmi1*$^{GFP/+}$ animals showed that cells with higher GFP expression (GFP^{HI}) produced significantly more colonies than cells with low GFP (GFP^{LO}) (Supplementary Fig. S3i,j). Together, these data supported the functional results and confirmed that *Bmi1* is required to maintain dental epithelial stem cells.

We then tested whether *Ink4a/Arf* deletion could rescue the colony-forming defect associated with loss of *Bmi1* activity by culturing LaCL cells from *Bmi1*$^{-/-}$*;Ink4a/Arf*$^{-/-}$ mice. In contrast to the *Bmi1* mutants, the dissociated *Bmi1*$^{-/-}$*;Ink4a/Arf*$^{-/-}$ LaCL cells readily formed colonies that were comparable in numbers to the control (Supplementary Fig. S3h), however the *Bmi1*$^{-/-}$*;Ink4a/Arf*$^{-/-}$ colonies contained larger cells (Fig. 4a,b). We reasoned that whereas *Bmi1*$^{-/-}$ cells normally cannot self-renew due to elevated *Ink4a/Arf* expression, deletion of the *Ink4a/Arf* locus enabled these cells to proliferate. The altered morphology in *Bmi1*$^{-/-}$*;Ink4a/Arf*$^{-/-}$ cells suggested that BMI1 additionally regulates a developmental program that is independent of *Ink4a/Arf* expression. Consistent with this notion, the transcriptomes of *Bmi1*$^{-/-}$*;Ink4a/Arf*$^{-/-}$ colonies were dramatically different from wild-type controls and very similar to *Bmi1*$^{-/-}$ colonies (Supplementary Fig. S4). Thus, BMI1 must additionally control cell morphology and differentiation by regulating the expression of other genes.

To test whether upregulation of *Hox* genes was an important contributor to the mutant phenotype in *Bmi1* null incisors, we used lentiviral transduction to introduce shRNAs against *Hoxa9* and *Hoxc9*. These genes were the most upregulated *Hox* family members in both *Bmi1*$^{-/-}$ and *Bmi1*$^{-/-}$*;Ink4a/Arf*$^{-/-}$ mutants as well as in colonies derived from these animals (Fig. 3a, Fig. 4 g,h). qPCR results demonstrated that the shRNAs effectively knocked down *Hoxa9* and *Hoxc9*, whereas control scrambled sequences did not (Fig. 4 g,h). Furthermore, the doubly-infected colonies exhibited morphology and cell size similar to controls (Fig. 4 a,c,f). The rescue by Hoxa9/c9 shRNAs coincided with upregulation of *Cdh1* (encoding E-cadherin) and *Itga6* and with downregulation of *Cdh3* (encoding P-cadherin), *Amtn*, and *Klk4* (Fig. 4 i–m, Supplementary Fig. S5c–g), although single knockdown of either Hox gene alone did not show a clear rescue (Supplementary Fig. S5h,i), most likely due to functional redundancy. Thus, reducing *Hoxa9/c9* expression reconstituted the incisor epithelial stem cell expression signature, which indicated that deregulated expression of *Hoxa9* and *Hoxc9* was at least partially responsible for the changes in stem cell morphology and gene expression in *Bmi1*$^{-/-}$ cells.

Repression of *Hox* genes in the adult dental stem cells is therefore an important function of *Bmi1*, and this finding led us to predict that overexpression of *Hox* genes in the LaCL would phenocopy the *Bmi1*$^{-/-}$ mutants. To that end, we first introduced exogenous *Hoxa9*/*c9* by lentiviral transduction into cultured control LaCL cells (Fig. 4e,g,h). This overexpression caused enlarged cell size, downregulated expression of *Cdh1* and *Itga6*, and upregulated *Amtn* and *Klk4* expression, all of which are characteristic of the *Bmi1*$^{-/-}$ mutants (Fig. 4f,i–m). However, *Cdh3* expression was not altered, suggesting that additional genes and/or factors were required for its upregulation. To further test whether *Hox* genes function similarly *in vivo*, we generated *Gli1*$^{CreER/+}$*;R26*$^{Hoxc9/YFP}$ mice, in which ectopic *Hoxc9*

Author Manuscript Author Manuscript Author Manuscript Author Manuscript

expression and a YFP Cre-reporter were induced specifically in the LaCL stem cells by tamoxifen injection (Fig. 5 a,f). Overexpression of *Hoxc9* led to downregulation of E-cadherin and ITGA6 in the SR and OEE and to expanded P-cadherin expression (Fig. 5b–d,g–i), matching the gene expression phenotype exhibited by the *Bmi1*$^{-/-}$ mutants, although LaCL size was not affected (Fig. 5e,j,k).

Together, these data demonstrate that *Bmi1*-positive cells in the LaCL are adult stem cells and that *Bmi1* function is required to maintain these cells through two distinct mechanisms (Fig. 5l). The first is via repression of *Ink4a*/*Arf* expression to permit stem cell self-renewal, a well-documented function of *Bmi1* in other systems[1, 3, 4]. However, the *Bmi1*$^{-/-}$ phenotype was not fully rescued by the deletion of *Ink4a/Arf*, and thus, prevention of arrested cell division is not the sole function of BMI1. We found that the second function of BMI1 is to suppress the expression of *Hox* genes to prevent inappropriate cell differentiation. A similar observation was made in the *Drosophila* testis, where mutated polycomb genes resulted in *Abdominal-B* upregulation and abnormal cyst stem cell differentiation[30], hinting at an evolutionarily conserved role for *Bmi1* in regulating stem cell differentiation. It is notable that upregulation of *Hox* genes has also been documented in other *Bmi1*$^{-/-}$ adult stem cells[1, 2, 5–7], and it will be important to consider the role of repression of *Hox* genes and other targets by BMI1 in those systems. For example, in haematopoietic stem cells, *Ebf1* and *Pax5*[14] regulate lineage specification, and their upregulation in *Bmi1* mutants causes a lineage shift during haematopoiesis. In the *Bmi1* null incisor, we observed upregulation of genes associated with maturing ameloblasts in addition to upregulation of *Hox* genes, which is likely the cause of the abnormal enamel deposition by *Bmi1*$^{-/-}$ ameloblasts. Thus, we propose that *Bmi1* has two distinct functions: (1) maintain adequate stem cell self-renewal by suppressing *Ink4a*/*Arf* and (2) prevent inappropriate differentiation by inhibiting the expression of *Hox* genes and other genes important for cellular maturation (Fig. 5i).

Methods

Mouse lines and injections

Mice carrying the Bmi1^{GFP} [15], Bmi1^{CreER} [18], Gli1^{CreER} [31], Gli1^{lacZ} [32], K5tTA[33], R26R-Tm-GFP [19], and *H2B-GFP*[16] alleles or transgenes were maintained and genotyped as previously described. For *R26*$^{Hoxc9/+}$, chicken (*Gallus gallus*) *Hoxc9* was cloned and inserted into the ROSA locus as described [34, 35]. PCR genotyping for the *R26*^{Hoxc9} allele was performed using the following primers: R26wt_FW: 5′-AAAGTCGCTCTGAGTTGTTAT-3′, R26wt_REV: 5′-GGAGCGGGAGAAATGGATATG-3′, and R26loxC9_REV: 5′-GTTATGTAACGCGGAACTCCA-3′. *Gli1*^{CreER};*R26*$^{Hoxc9/YFP}$ mice were subsequently generated by mating *Gli1*$^{CreER/+}$;*R26*$^{YFP/+}$ male to *R26*$^{Hoxc9/Hoxc9}$ females. For lineage-tracing studies, 5 mg Tamoxifen dissolved in corn oil was injected IP into adult mice between 8 and 12 weeks of age at 5 mg per 25 g body weight. For label retention studies, postnatal day 2 animals were injected with 200 μg BrdU for 3 consecutive days and sacrificed after 6 weeks. At least three mice were examined at each time point for all experiments. Unless specified in the main text, 6-week-old mice were used. Both male and female mice were included in this study.

Author Manuscript Author Manuscript Author Manuscript Author Manuscript

Lentiviral production and colony forming assay

All shRNAs were designed using pSicoOligomaker 1.5 and cloned into the pSicoR-GFP vector (Tyler Jacks lab protocols, http://web.mit.edu/jacks-lab/protocols_table.html). Two sets of shRNAs against Hoxa9 and Hoxc9 were designed. The antisense sequences are: *Hoxa9* (1st set): TTAATGCCATAAGGCCGGC, *Hoxa9* scrambled (1st set): TACTATCGGTAACGGACGC, *Hoxa9* (2nd set): TAAACAGAAACTCCTTCTC, *Hoxa9* scrambled (2nd set): AGTCTACAACTATTCACAC, *Hoxc9* (1st set): ATTGAAGAGAAACTCCTTC, *Hoxc9* scrambled (1st set): ACATGAATTAAGTTCCGAC, *Hoxc9* (2nd set): ATAGACCACAGACGACTGC, *Hoxc9* scrambled (2nd set): ACGTACGAGAAACAGCTCC. Lentiviral packaging was performed using a 3rd generation packaging system (Addgene) according to established protocols. The *in vitro* culture system was modeled after a system for culture of hair follicle stem cells[36–38] and has been previously published[29]. Briefly, whole incisors, including the entire dental epithelium, were isolated from mandibles and incubated in collagenase (Worthington) for 4 hours on ice. Labial cervical loops were mechanically isolated and dissociated in 100 μl Accumax (Sigma) at 37°C for 1 hour using gentle pippetting. Cells were counted and plated at a density of 15,000 cells per well on a 6 well plate. Colonies were then either harvested for RNA extraction or counted and imaged on a Leica inverted microscope after 10 days. All experiments were performed at least three times. Colony forming efficiency was expressed as a ratio of the number of small-cell containing colonies divided by the total number of plated cells. Cell sizes were measured using ImageJ (n = 3 independent experiments, and 100 cells were scored for each experiment).

Flow cytometry

LaCLs from *Bmi1*$^{GFP/+}$ and *Bmi1*$^{+/+}$ mice were isolated and dissociated as described above. Single cell suspensions were sorted for GFP expression using a FACSAria 2 cell sorter (BD Biosciences) at the Eli and Edythe Broad Center of Regeneration Medicine and Stem Cell Research at UCSF, Cell Analysis core. Two separate experiments were performed.

3D reconstruction of cervical loops

The epithelium was outlined from ~40 consecutive 7 μm thick coronal sections at the most proximal end of the mouse incisor (n = 4 animals per genotype). BioVis software (http://www.biovis3d.com) was used to generate 3-dimensional (3D) reconstructions from this data and to calculate the volume of the structures.

Microarray analysis and qPCR

Total RNA from dissected whole LaCLs or colonies was extracted using the Ambion Mirvana RNA Isolation kit. Sample preparation, labeling, and array hybridizations were performed according to standard protocols from the UCSF Shared Microarray Core Facilities and Agilent Technologies (http://www.arrays.ucsf.edu and http://www.agilent.com). Total RNA quality was assessed using a Pico Chip on an Agilent 2100 Bioanalyzer (Agilent Technologies, Palo Alto, CA). The datasets were normalized using the *quantile* normalization method[39]. No background subtraction was performed, and the median feature pixel intensity was used as the raw signal before normalization. A one-way

Author Manuscript Author Manuscript Author Manuscript Author Manuscript

ANOVA linear model was fit to the comparison to estimate the mean M values and calculate moderated t-statistic, B statistic, false discovery rate, and p-value for each gene for the comparison of interest. All procedures were carried out using functions in the R package *limma in Bioconductor*. Gene ontology analysis was performed using the Term Enrichment tool in AmiGO (http://amigo.geneontology.org). For qPCR analysis, cDNA was generated using the Advantage RT for PCR kit (Clontech), and Taqman assays (Ambion) were used to perform qPCR. Primers for *Hoxc9*, *Amtn*, *Klk4*, and *L19* were ordered from IDT PrimeTime. Primer sequences for *Hoxa9*, *Cdh1*, *Cdh3*, and *Itga6* are:*Hoxa9*: forward-GAATGAGAGCGGCGGAGAC, reverse- GAGCGAGCATGTAGCCAGTTG, *Cdh1*: forward- AATGAAGCCCCCATCTTTAT, reverse- GAGATGGACAGAGAAGACGC, *Cdh3*: forward-CCGCATCTTAAGGAGACGAA, reverse-AAATCTTGGTGCCTCTGTCC, *Itga6*: forward- GGAGCCTCTTCGGCTTCTC, reverse-AGTGCTTCTGCCCGAGGT. All samples were normalized to L19. CT values were extracted, and relative gene expression levels were calculated using the ΔΔCT method. All experiments were performed at least three times.

Histology and Immunofluorescence

Jaws were dissected from perfusion-fixed animals, post-fixed in 4% PFA overnight, decalcified in RNase-free 0.5 M EDTA for 16 days, and processed for paraffin embedding. 7 μm sections were prepared and stained with Hematoxylin and Eosin using standard methods. For all images shown, representative samples were chosen after sectioning through the entire jaw, in order to avoid plane of section artifacts. Brightfield images were obtained using a Leica DFC 500 camera with a Leica DM 5000B microscope. For immunostaining, paraffin sections were rehydrated, incubated in 1mM EDTA just below boiling temperature for 30 min for antigen retrieval, washed in distilled H_2O, and treated for 20 min with 3% H_2O_2 in PBS. Primary antibodies against GFP (1:5000, Torrey Pines, TP401), E-cadherin (1:1000, Invitrogen,131900), P-cadherin (1:1000, Invitrogen,132000Z), BrdU (1:500, Abcam, ab6326), and ITGA6 (1:1000, Santa Cruz, sc-10730) were used. Washes in PBS (3 × 20 min) and PBS-T (1 × 5 min) were followed by incubation with Alexa fluor 488 and 555 secondary antibodies (1:500, Invitrogen) or biotinylated anti-rat secondary antibody (Vector BA-4001) followed by signal amplification (Perkin Elmer). Sections were counterstained with DAPI (Vector Laboratories) and mounted in 1% DABCO in glycerol. Images were acquired using a Leica-TCS SP5 confocal microscope. BrdU staining was quantified using ImageJ. TUNEL staining was performed according to the manufacturer's protocol (Roche 12156792910). All experiments were performed at least three times.

MicroCT analysis

Hemimandibles (n = 3 per genotype) were imaged under wet conditions using a Micro XCT (Xradia, Pleasanton, CA) at a 2X magnification using a tungsten anode setting of 90keV and 66 microamps. Virtual sections from reconstructed tomographs were used to study the X-ray attenuation of incisor enamel across groups under identical experimental parameters and at similar sectioning planes.

Author Manuscript Author Manuscript Author Manuscript Author Manuscript

Statistical analysis

For statistical analyses, mean values with standard deviation (s.d.) are shown in most graphs. All experiments were performed independently at least three times, and the exact n numbers are listed in the figure legends. *P* values were obtained from student t-tests with paired samples. P<0.05 was determined to be significant for all experiments. Actual *P* values are shown in each figure or figure legend.

Accession Codes

Gene Expression Omnibus: GSE46001

Supplementary Material

Refer to Web version on PubMed Central for supplementary material.

Acknowledgments

We thank members of the Klein laboratory for helpful advice, Fred Michon for discussion, D.-K. Tran and S. Alto for technical assistance, X.-P. Wang for help with the culture system, Andrea Barczak and the UCSF Microarray Core Facilities for help with experiments and analysis, and Irving Weissman for mice. This work was supported by R01-DE021420 (NIH/NIDCR) and a CIRM New Faculty Award II, both to O. D. Klein.

References

1. Molofsky AV, et al. Bmi-1 dependence distinguishes neural stem cell self-renewal from progenitor proliferation. Nature. 2003; 425:962–967. [PubMed: 14574365]
2. Park IK, et al. Bmi-1 is required for maintenance of adult self-renewing haematopoietic stem cells. Nature. 2003; 423:302–305. [PubMed: 12714971]
3. Jacobs JJ, Kieboom K, Marino S, DePinho RA, van Lohuizen M. The oncogene and Polycomb-group gene bmi-1 regulates cell proliferation and senescence through the ink4a locus. Nature. 1999; 397:164–168. [PubMed: 9923679]
4. Molofsky AV, He S, Bydon M, Morrison SJ, Pardal R. Bmi-1 promotes neural stem cell self-renewal and neural development but not mouse growth and survival by repressing the p16Ink4a and p19Arf senescence pathways. Genes Dev. 2005; 19:1432–1437. [PubMed: 15964994]
5. Zacharek SJ, et al. Lung stem cell self-renewal relies on BMI1-dependent control of expression at imprinted loci. Cell Stem Cell. 2011; 9:272–281. [PubMed: 21885022]
6. Bruggeman SW, Hulsman D, van Lohuizen M. Bmi1 deficient neural stem cells have increased integrin dependent adhesion to self-secreted matrix. Biochim Biophys Acta. 2009; 1790:351–360. [PubMed: 19298843]
7. Fasano CA, et al. shRNA knockdown of Bmi-1 reveals a critical role for p21-Rb pathway in NSC self-renewal during development. Cell Stem Cell. 2007; 1:87–99. [PubMed: 18371338]
8. Harada H, et al. Localization of putative stem cells in dental epithelium and their association with Notch and FGF signaling. The Journal of cell biology. 1999; 147:105–120. [PubMed: 10508859]
9. Wang XP, et al. An integrated gene regulatory network controls stem cell proliferation in teeth. PLoS Biol. 2007; 5:e159. [PubMed: 17564495]
10. Klein OD, et al. An FGF signaling loop sustains the generation of differentiated progeny from stem cells in mouse incisors. Development. 2008; 135:377–385. [PubMed: 18077585]
11. Smith CE, Warshawsky H. Cellular renewal in the enamel organ and the odontoblast layer of the rat incisor as followed by radioautography using 3H-thymidine. Anat Rec. 1975; 183:523–561. [PubMed: 1200409]
12. Seidel K, et al. Hedgehog signaling regulates the generation of ameloblast progenitors in the continuously growing mouse incisor. Development. 2010; 137:3753–3761. [PubMed: 20978073]

Author Manuscript Author Manuscript Author Manuscript Author Manuscript

13. Juuri E, et al. Sox2+ stem cells contribute to all epithelial lineages of the tooth via Sfrp5+ progenitors. Developmental cell. 2012; 23:317–328. [PubMed: 22819339]
14. Oguro H, et al. Poised lineage specification in multipotential hematopoietic stem and progenitor cells by the polycomb protein Bmi1. Cell Stem Cell. 2010; 6:279–286. [PubMed: 20207230]
15. Hosen N, et al. Bmi-1-green fluorescent protein-knock-in mice reveal the dynamic regulation of bmi-1 expression in normal and leukemic hematopoietic cells. Stem Cells. 2007; 25:1635–1644. [PubMed: 17395774]
16. Tumbar T, et al. Defining the epithelial stem cell niche in skin. Science. 2004; 303:359–363. [PubMed: 14671312]
17. Joyner AL, Zervas M. Genetic inducible fate mapping in mouse: establishing genetic lineages and defining genetic neuroanatomy in the nervous system. Dev Dyn. 2006; 235:2376–2385. [PubMed: 16871622]
18. Sangiorgi E, Capecchi MR. Bmi1 is expressed in vivo in intestinal stem cells. Nat Genet. 2008; 40:915–920. [PubMed: 18536716]
19. Muzumdar MD, Tasic B, Miyamichi K, Li L, Luo L. A global double-fluorescent Cre reporter mouse. Genesis. 2007; 45:593–605. [PubMed: 17868096]
20. Sangiorgi E, Capecchi MR. Bmi1 lineage tracing identifies a self-renewing pancreatic acinar cell subpopulation capable of maintaining pancreatic organ homeostasis. Proc Natl Acad Sci U S A. 2009; 106:7101–7106. [PubMed: 19372370]
21. Li CY, et al. E-cadherin regulates the behavior and fate of epithelial stem cells and their progeny in the mouse incisor. Dev Biol. 2012; 366:357–366. [PubMed: 22537490]
22. Hwang WS, Tonna EA. Autoradiographic Analysis of Labeling Indices and Migration Rates of Cellular Component of Mouse Incisors Using Tritiated Thymidine (H3tdr). J Dent Res. 1965; 44:42–53. [PubMed: 14245495]
23. Ramalho-Santos M, Yoon S, Matsuzaki Y, Mulligan RC, Melton DA. “Stemness”: transcriptional profiling of embryonic and adult stem cells. Science. 2002; 298:597–600. [PubMed: 12228720]
24. Rock JR, et al. Basal cells as stem cells of the mouse trachea and human airway epithelium. Proc Natl Acad Sci U S A. 2009; 106:12771–12775. [PubMed: 19625615]
25. Tani H, Morris RJ, Kaur P. Enrichment for murine keratinocyte stem cells based on cell surface phenotype. Proc Natl Acad Sci U S A. 2000; 97:10960–10965. [PubMed: 11005869]
26. Xiong J, Mrozik K, Gronthos S, Bartold PM. Epithelial Cell Rests of Malassez Contain Unique Stem Cell Populations Capable of Undergoing Epithelial-Mesenchymal Transition. Stem Cells Dev. 2012
27. Simmer JP, Richardson AS, Smith CE, Hu Y, Hu JC. Expression of kallikrein-related peptidase 4 in dental and non-dental tissues. European journal of oral sciences. 2011; 119 (Suppl 1):226–233. [PubMed: 22243250]
28. Iwasaki K, et al. Amelotin--a Novel Secreted, Ameloblast-specific Protein. Journal of dental research. 2005; 84:1127–1132. [PubMed: 16304441]
29. Chavez MG, et al. Characterization of dental epithelial stem cells from the mouse incisor with two-dimensional and three-dimensional platforms. Tissue engineering Part C, Methods. 2013; 19:15–24. [PubMed: 22742471]
30. Morillo Prado JR, Chen X, Fuller MT. Polycomb group genes Psc and Su(z)2 maintain somatic stem cell identity and activity in Drosophila. PloS one. 2012; 7:e52892. [PubMed: 23285219]
31. Ahn S, Joyner AL. Dynamic changes in the response of cells to positive hedgehog signaling during mouse limb patterning. Cell. 2004; 118:505–516. [PubMed: 15315762]
32. Bai CB, Auerbach W, Lee JS, Stephen D, Joyner AL. Gli2, but not Gli1, is required for initial Shh signaling and ectopic activation of the Shh pathway. Development. 2002; 129:4753–4761. [PubMed: 12361967]
33. Diamond I, Owolabi T, Marco M, Lam C, Glick A. Conditional gene expression in the epidermis of transgenic mice using the tetracycline-regulated transactivators tTA and rTA linked to the keratin 5 promoter. J Invest Dermatol. 2000; 115:788–794. [PubMed: 11069615]
34. Sousa VH, Miyoshi G, Hjerling-Leffler J, Karayannis T, Fishell G. Characterization of Nkx6-2-derived neocortical interneuron lineages. Cerebral cortex. 2009; 19 (Suppl 1):i1–10. [PubMed: 19363146]

Author Manuscript Author Manuscript Author Manuscript Author Manuscript

35. Jung H, et al. Global control of motor neuron topography mediated by the repressive actions of a single hox gene. Neuron. 2010; 67:781–796. [PubMed: 20826310]

36. Rochat A, Kobayashi K, Barrandon Y. Location of stem cells of human hair follicles by clonal analysis. Cell. 1994; 76:1063–1073. [PubMed: 8137423]

37. Blanpain C, Lowry WE, Geoghegan A, Polak L, Fuchs E. Self-renewal, multipotency, and the existence of two cell populations within an epithelial stem cell niche. Cell. 2004; 118:635–648. [PubMed: 15339667]

38. Barrandon Y, Green H. Three clonal types of keratinocyte with different capacities for multiplication. Proc Natl Acad Sci U S A. 1987; 84:2302–2306. [PubMed: 2436229]

39. Bolstad BM, Irizarry RA, Astrand M, Speed TP. A comparison of normalization methods for high density oligonucleotide array data based on variance and bias. Bioinformatics. 2003; 19:185–193. [PubMed: 12538238]

Author Manuscript Author Manuscript Author Manuscript Author Manuscript

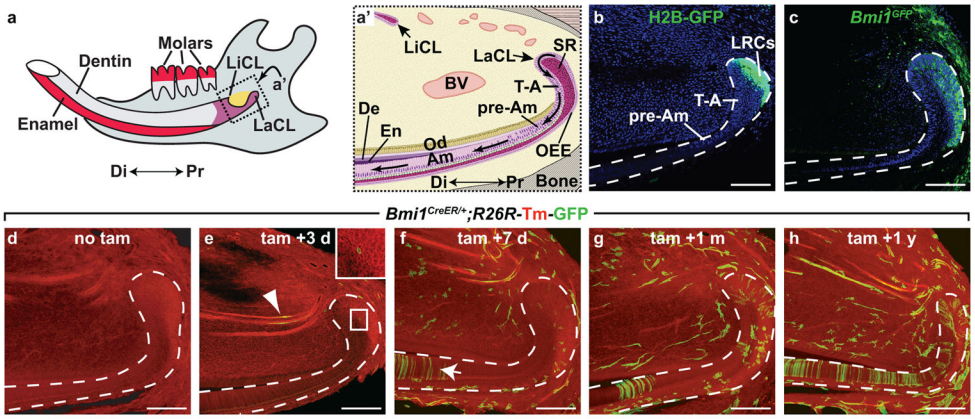

Figure 1. *Bmi1*-expressing cells in the dental epithelium are stem cells

(**a**) Schematic diagram of an adult mandible. The incisor is a long tooth that grows under the molars. Enamel is produced by ameloblasts, which are present only on the labial surface. Dentin, produced by odontoblasts, is deposited on both the labial and lingual surfaces. Di, distal. LiCL, lingual cervical loop. LaCL, labial cervical loop. Pr, proximal. (**a′**) Schematic representation of the cell types associated with the dental epithelium and stem cell niche. Arrows in labial epithelium represent direction of movement of cells as they differentiate. Am, ameloblasts. BV, blood vessel. De, dentin. En, enamel. Od, odontoblasts. OEE, outer enamel epithelium. pre-AM, pre-ameloblasts. SR, stellate reticulum. T-A, transit amplifying. (**b**) *K5tTA;H2BGFP* mice treated for 2 months with doxycycline reveal label retention in the SR and OEE of the labial cervical loop. LRC, label retaining cells. (**c**) $Bmi1^{GFP}$ expression is localized to the OEE and SR of the cervical loop. (**d**–**h**) $Bmi1^{CreER}$*;R26R-Tm-GFP* mice were induced at 6 weeks with tamoxifen and chased for the indicated time period. Dotted lines in b–h outline the dental epithelium. Scale bar = 100 μm.

Author Manuscript Author Manuscript Author Manuscript Author Manuscript

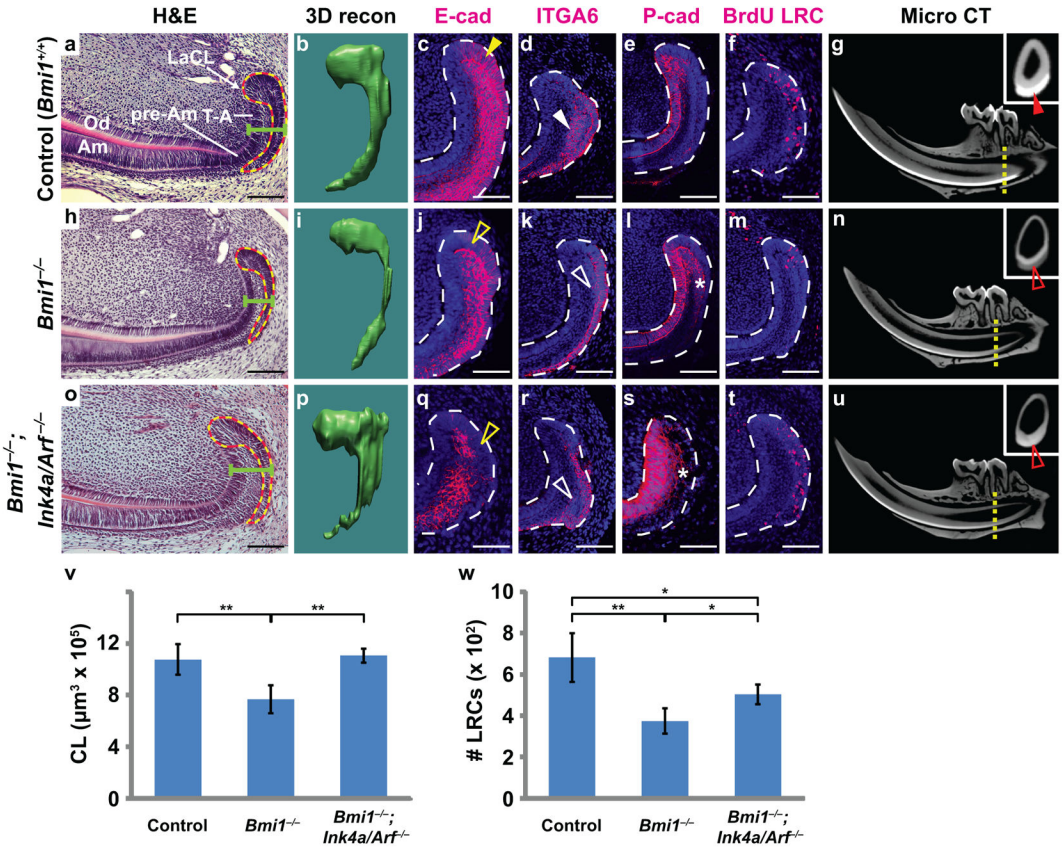

Figure 2. Deletion of *Bmi1* affects adult LaCL through both *Ink4a*/*Arf*-dependent and independent mechanisms

(**a**,**h**,**o**) Haematoxylin and eosin staining comparing LaCLs from 5-month-old control (*Bmi1*$^{+/+}$), *Bmi1*$^{-/-}$, and *Bmi1*$^{-/-}$;*Ink4a/Arf*$^{-/-}$ mice. Dotted lines outline region traced on coronal sections for 3-dimensional (3D) renderings. Green bar demarcates width of cervical loop. (**b**,**i**,**p**) 3D renderings enable reconstruction (recon) of the control, *Bmi1*$^{-/-}$ and *Bmi1*$^{-/-}$;*Ink4a/Arf*$^{-/-}$ (triple mutant) LaCLs. (**c**,**j**,**q**) E-cadherin staining of the LaCL in control, *Bmi1*, and triple mutants. E-cadherin expression is downregulated in both the single and triple mutants (open yellow arrowheads) when compared to the control (yellow arrowhead). (**d**,**k**,**r**) Expression of ITGA6 detected by immunostaining is decreased in the *Bmi1*$^{-/-}$ and *Bmi1*$^{-/-}$;*Ink4a/Arf*$^{-/-}$ LaCLs (open white arrowheads) compared to the control (white arrowhead). (**e**,**l**,**s**) P-cadherin expression in the LaCL is expanded in both the *Bmi1* and *Bmi1*$^{-/-}$;*Ink4a/Arf*$^{-/-}$ LaCLs (asterisks). (**f**,**m**,**t**) Representative sections of LaCLs from control, *Bmi1*$^{-/-}$, and *Bmi1*$^{-/-}$;*Ink4a/Arf*$^{-/-}$ jaws. Animals were pulsed with BrdU post-natally and aged for 1.5 months for identification of label-retaining cells (LRCs). (**g**,**n**,**u**) MicroCT scans showing mandibles from 5-month-old control, *Bmi1*$^{-/-}$ and *Bmi1*$^{-/-}$;*Ink4a/Arf*$^{-/-}$ mice. Enamel is thinner and less mineralized in both single and triple mutants when compared to the control. Insets are coronal sections through the distal root of the second molar (yellow dotted lines) and show that enamel is less mineralized in mutants (open red arrowheads) than in the control (red arrowhead). (**v**) Quantification of volume of the LaCL stem cell compartment in control, *Bmi1*$^{-/-}$, and *Bmi1*$^{-/-}$;*Ink4a/Arf*$^{-/-}$ (n = 4 mice for each genotype). (**w**) Quantification of BrdU LRCs by sectioning and staining through the

Author Manuscript Author Manuscript Author Manuscript Author Manuscript

entire LaCL (n = 5 control, 3 *Bmi1*$^{-/-}$, and 4 *Bmi1*$^{-/-}$*;Ink4a/Arf*$^{-/-}$ mice). Error bars indicate means ± s.d. * is $p < 0.05$, and ** is $p < 0.001$. Scale bar = 100 μm for **a**,**h**,**o**, and 75 μm for **c**–**f**, **j**–**m**, and **q**–**t**. Source data of statistical analyses are shown in Supplementary Table S2 and S3.

Author Manuscript Author Manuscript Author Manuscript Author Manuscript

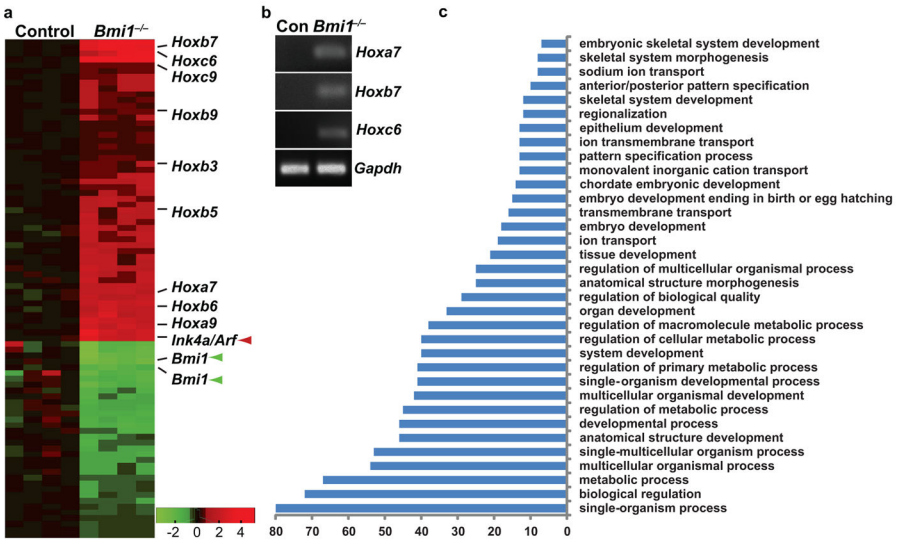

Figure 3. *Bmi1* suppresses expression of *Ink4a*/*Arf* and *Hox* genes

(**a**) Microarray analysis on *Bmi1*$^{+/+}$ (control or con) and *Bmi1*$^{-/-}$ dental epithelia shows that inactivation of *Bmi1* leads to de-regulation of several *Hox* genes, in addition to *Ink4a/Arf* (red arrowhead). Loss of *Bmi1* expression is indicated by green arrowheads. (**b**) RT-PCR analysis showing upregulation of *Hoxa7*, *b7*, and *c6* in *Bmi1*$^{-/-}$ LaCLs. (**c**) Gene ontology analysis reveals upregulation of genes normally involved in developmental processes and cell differentiation.

Author Manuscript Author Manuscript Author Manuscript Author Manuscript

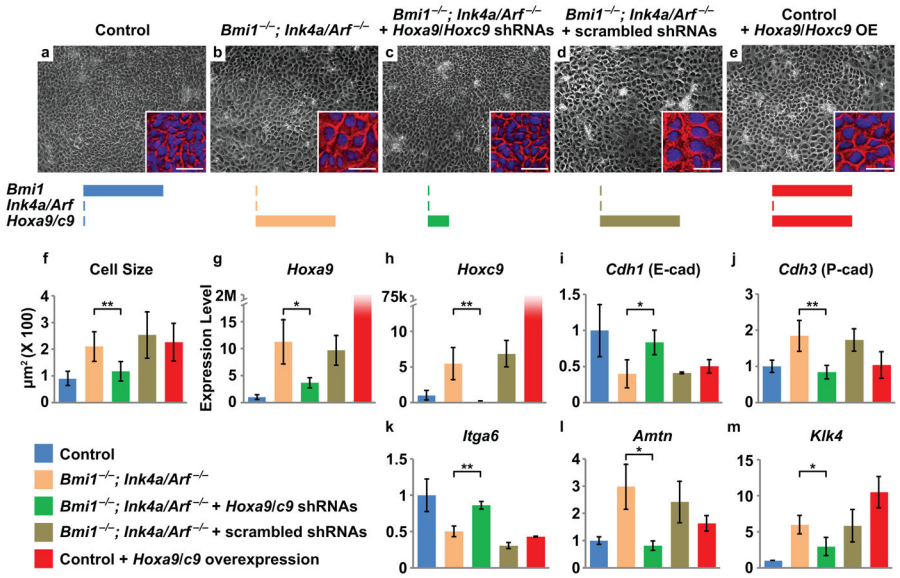

Figure 4. *Hox* gene upregulation contributes to the *Bmi1* loss of function phenotype

(**a**) Stem cell colonies derived from control LaCLs are composed of small, rounded cells. (**b**) Deletion of *Ink4a/Arf* enables colony formation by $Bmi1^{-/-}$ cells, but cell size is increased. (**c**) Knockdown of *Hoxa9* and *Hoxc9* rescues the morphological defects in $Bmi1^{-/-}$;$Ink4a/Arf^{-/-}$ colonies. (**d**) Scrambled shRNA does not rescue the phenotype. (**e**) Overexpression of *Hoxa9* and *Hoxc9* in control cells phenocopies the morphology of $Bmi1^{-/-}$;$Ink4a/Arf^{-/-}$ colonies. Insets in **a**–**e** are enlarged images of representative cells with pseudo-colored cell boundary (red) and DAPI nuclear staining (blue). Schematics represent the level of expression for each gene. (**f**) Quantification of cell size under different conditions (n = 3 independent experiments with 100 cells scored for each experiment). (**g**–**m**) Relative expression level by qPCR of *Hoxa9*, *Hoxc9*, *Cdh1*, *Cdh3*, *Itga6*, *Amtn*, and *Klk4* in cells cultured under different conditions (n = 3 independent experiments). Error bars indicate means ± s.d. * is $p < 0.05$, and ** is $p < 0.001$. Scale bar = 100 μm for **a**–**e** and 30 μm for the insets. Source data of statistical analyses are shown in Supplementary Table S4 and S5.

Author Manuscript Author Manuscript Author Manuscript Author Manuscript

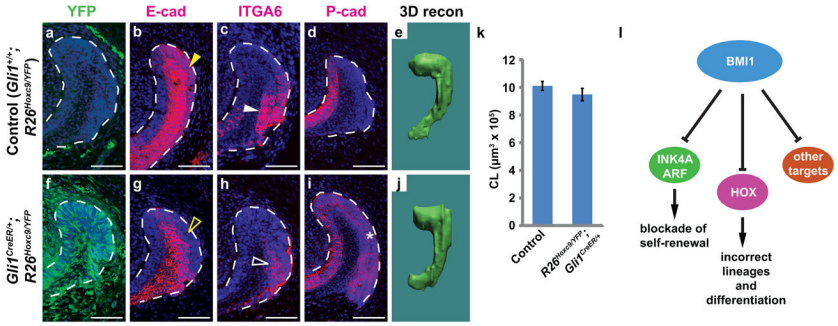

Figure 5. Overexpression of *Hoxc9* in LaCLs phenocopies *Bmi1* mutants

(**a**,**f**) *Hoxc9* and YFP Cre-reporter were overexpressed using a *Gli1*^{CreER} driver in the LaCL by tamoxifen induction, but not in the absence of Cre. YFP expression is shown here 10 days after induction. (**b**,**g**) E-cadherin is expressed in SR and OEE in the control LaCL (yellow arrowhead) but downregulated in the mutant (open yellow arrowhead). (**c**,**h**) ITGA6 is similarly downregulated in the mutant (compare solid and open white arrowheads). (**d**,**i**) P-cadherin expression is restricted in the T-A region in the control but expanded in the mutant (asterisk). All LaCLs are outlined by white dashed lines. Scale bar = 75 µm. (**e**,**j**,**k**) 3D reconstruction (recon) of LaCLs shows no difference in LaCL size between control and *Gli1*$^{CreER/+}$;*R26*$^{Hoxc9/YFP}$ (n = 3 animals for each genotype). Error bars indicate means ± s.d. Source data of statistical analysis are shown in Supplementary Table S2. (**i**) Model for function of BMI1 in incisor stem cells.